Available online at www.sciencedirect.com
ScienceDirect
Ceramics International 37 (2011) 651–658
CERAMICS INTERNATIONAL
www.elsevier.com/locate/ceramint

The white porcelains from Dehua kiln site of China. Part II: Microstructure and its physicochemical basis

Weidong Li [a,b,*], Hongjie Luo [a,b], Jianan Li [c], Xiaoke Lu [a,b], Jingkun Guo [a,b]

[a] Shanghai Institute of Ceramics, Chinese Academy of Sciences, Shanghai 200050, China
[b] Key Scientific Research Base of Ancient Ceramics, State Administration for Cultural Heritage, China
[c] The Museum of Fujian Province, Fuzhou, Fujian 350001, China

Received 25 May 2010; received in revised form 27 August 2010; accepted 14 October 2010
Available online 18 November 2010

Abstract

Dehua is one of the most famous white porcelain production areas and one of the main porcelain exporting centers in Southern China. In this part of the study, white porcelain samples from the Song to Qing Dynasties excavated from Wanpinglun, Qudougong, Zulonggong, Jiabeishan and Xingjiao kiln sites were analyzed to investigate microstructure and its physicochemical basis. Physical properties of the samples were also studied, to evaluate the quality of porcelain production of Dehua kiln in ancient times.

Keywords: Dehua kiln; White porcelain; Microstructure; Physicochemical basis

1. Introduction

Dehua is one of the most famous white porcelain production areas and one of the main porcelain exporting centers in Southern China. Dehua kiln takes a very important position in ancient Chinese ceramics history.

White porcelain of Dehua kiln is distinguished in shape, appearance, decoration and technology. The kiln structure of Dehua also has its own characteristics and evolution regularity. More than 200 kiln sites from the Song Dynasty (960–1279 A.D.) to the Qing Dynasty (1644–1911 A.D.) have been discovered within the boundaries of Dehua county. Archaeological excavations were carried out on five Dehua kiln sites, including Wangpinglun, Qudougong, Zulonggong, Jiabeishan and Xingjiao kiln sites.

As for the visual appearance, Blanc de chine of the Ming Dynasty has the best quality, which is noted for its ivory white, mild and translucent glaze, well-sintered and translucent body. While the white porcelains of the Song, Yuan and Qing Dynasties are slightly inferior. Microstructure has a great influence on the visual appearance of Dehua white porcelain. In this part of the study, white porcelain samples excavated from Wanpinglun, Qudougong, Zulonggong, Jiabeishan and Xingjiao kiln sites were analyzed to investigate microstructure and its physicochemical basis of the white porcelains of the Song, Yuan, Ming, Qing Dynasties. Physical properties of the samples were also studied, to evaluate the quality of porcelain production of Dehua kiln in ancient times.

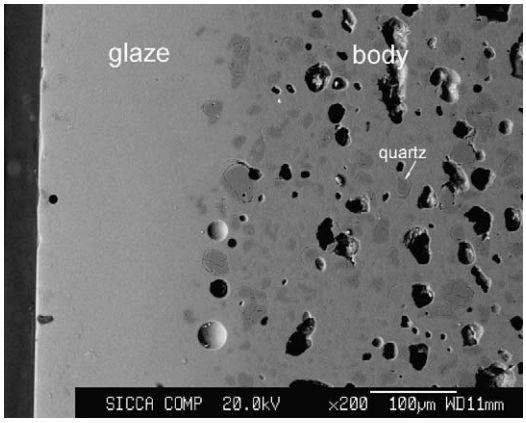

Fig. 1. SEM image of the cross-section of white porcelain 5-32 from Wangpinglun kiln site, the Song Dynasty. A homogenous glaze layer with no crystals, many dissociative quartz particles in body.

* Corresponding author at: Shanghai Institute of Ceramics, Chinese Academy of Sciences, Shanghai 200050, China. Tel.: +86 21 52412373; fax: +86 21 52413903.
E-mail address: liwd@mail.sic.ac.cn (W. Li).

0272-8842/$36.00
doi:10.1016/j.ceramint.2010.10.029

Table 1
Microstructure characteristics of Dehua white porcelain.

Number	Kiln site	Time	Glaze	Body–glaze interaction layer
5-32	Wanpinglun	Song	No crystal	No interaction layer
5-2	Wanpinglun	Song	No crystal	No interaction layer
1-1	Zulonggong	Yuan	No crystal	A sparse interaction layer of short column-like crystals
1-41	Zulonggong	Yuan	No crystal	A sparse interaction layer of column-like crystals
3-4	Jiabeishan	Yuan	No crystal	No interaction layer
3-25	Jiabeishan	Yuan	No crystal	No interaction layer
6-32	Qudougong	Yuan	A few quartz crystals	A sparse interaction layer of column-like crystals
6-55	Qudougong	Yuan	No crystal	A sparse interaction layer of short column-like crystals
2-3	Zulonggong	Ming	A few short column-like crystals, a few quartz crystals	A dense interaction layer of short column-like crystals
2-25	Zulonggong	Ming	A few quartz crystals	A dense interaction layer of short column-like crystals
4-10	Jiabeishan	Ming	A few quartz crystals	A dense interaction layer of column-like crystals
4-26	Jiabeishan	Ming	A few quartz crystals	A dense interaction layer of short column-like crystals
7-13	Xingjiao	Qing	Many quartz crystals	No interaction layer
7-14	Xingjiao	Qing	Many quartz crystals	No interaction layer

2. Experimental

X-ray diffraction (Rigaku D/max 2550V, Japan) using Cu-Ka radiation was employed to identify the crystalline phases in body. Microstructure and micro-area composition was studied using electron probe microanalyzer (Shimadzu EPMA-8705QH2, Japan) and field emission transmission electron microscope equipped with EDS (JEOL JEM-2100F, Japan). Firing temperature of body was examined by dilatometer (NETZSCH DIL 402 C, Germany). Chromaticity was analyzed by Spectrophotometer (MINOLTA CM-700d, Japan). Bending strength of body was tested by universal testing machine (SATEC Instron-5592, USA). Apparent porosity, water absorption and bulk density of body were measured according to the corresponding national standard [1].

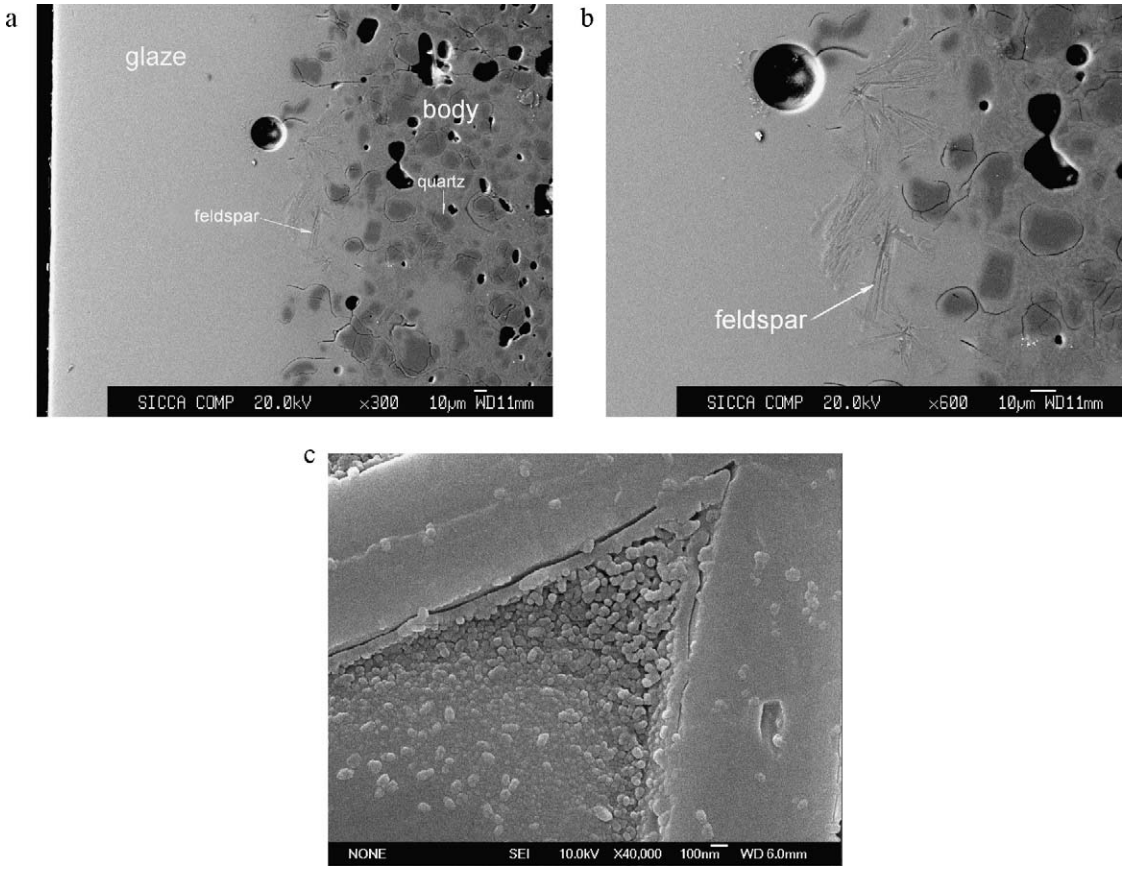

Fig. 2. SEM images of the cross-section of white porcelain 1-41 from Zulonggong kiln site, the Yuan Dynasty: (a) a homogenous glaze layer with no crystals, many dissociative quartz particles in body, (b) a sparse interaction layer of column-like crystals at body–glaze boundary, (c) phase-separation structure within the interspaces of crystals in the interaction layer.

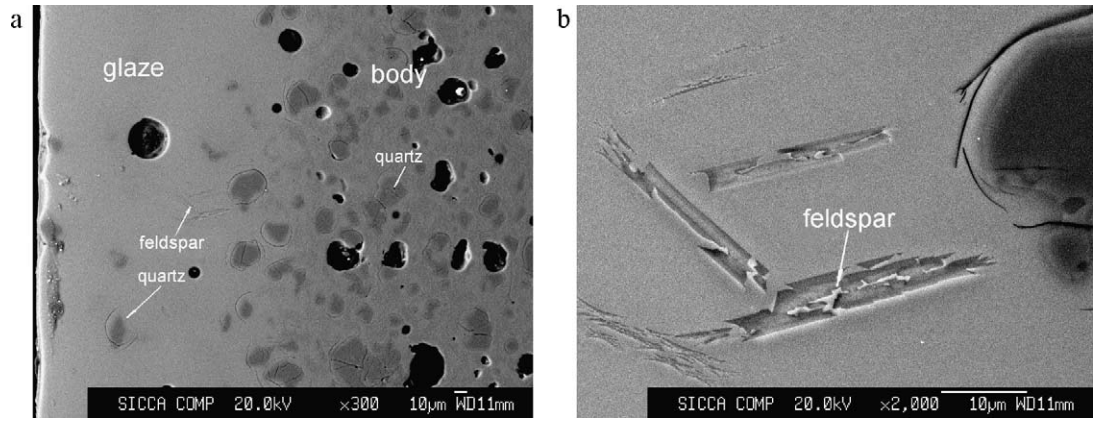

Fig. 3. SEM images of the cross-section of white porcelain 6-32 from Qudougong kiln site, the Yuan Dynasty: (a) a few quartz in glaze, many dissociative quartz particles in body and (b) a sparse interaction layer of column-like crystals at body–glaze boundary.

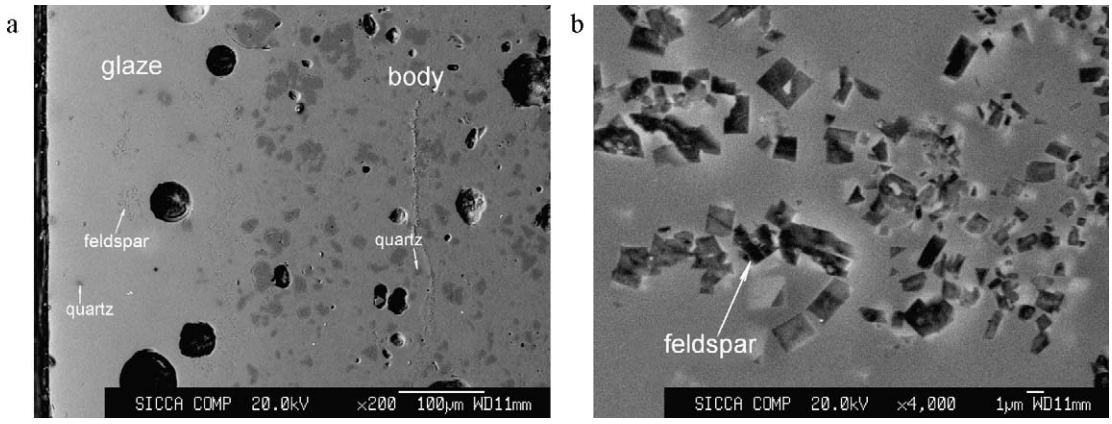

Fig. 4. SEM images of the cross-section of white porcelain 2-3 from Zulonggong kiln site, the Ming Dynasty: (a) a few quartz and short-column like crystals in glaze, many dissociative quartz particles in body and (b) a dense interaction layer of short column-like crystals at body–glaze boundary.

3. Results and discussion

3.1. Microstructure and its physicochemical basis

Some microstructure characteristics of the samples are given in Table 1. SEM images of the cross-sections are shown in Figs. 1–8. TEM images of the argon ion thinned body samples are presented in Figs. 10 and 11.

There are no or just a few un-melted dissociate quartz crystals in the Song, Yuan and Ming glaze layers, indicating that the technique for elutriating the glaze-used porcelain stones is rather fine during that time. But the elutriation technique is quite rough in the Qing Dynasty, many dissociative quartz particles with melting rims can be observed in glaze layers (Figs. 7 and 8). There are always many un-melted dissociate quartz particles, 10–100 μm in diameter, present in

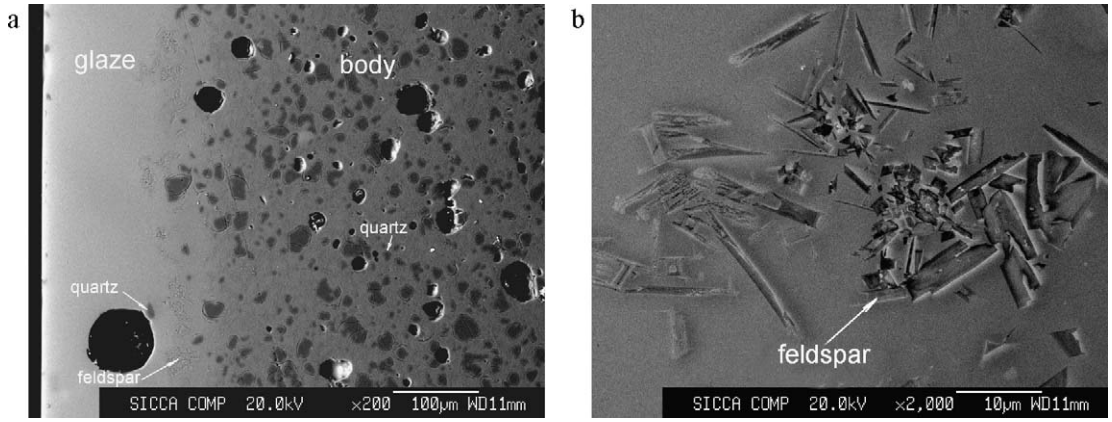

Fig. 5. SEM images of the cross-section of white porcelain 4-10 from Jiabeishan kiln site, the Ming Dynasty: (a) a few quartz in glaze, many dissociative quartz particles in body and (b) a dense interaction layer of column-like crystals at body–glaze boundary.

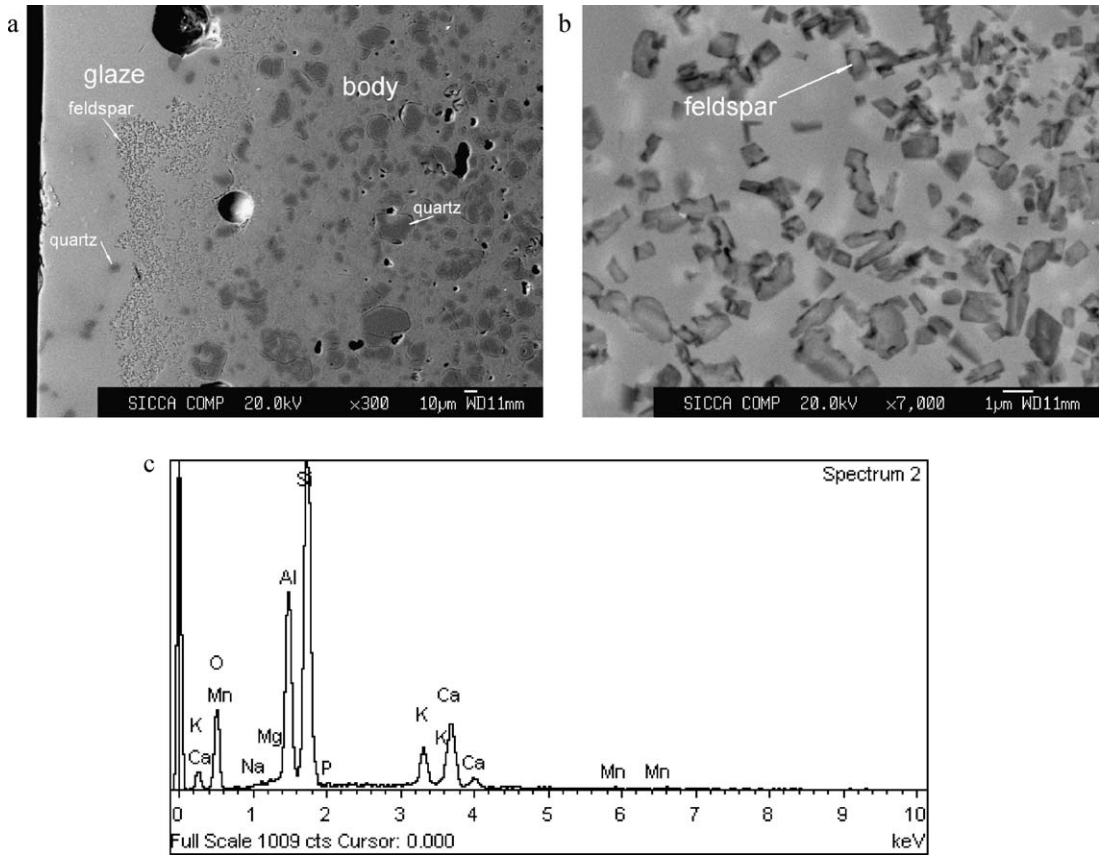

Fig. 6. SEM images of the cross-section of white porcelain 4-26 from Jiabeishan kiln site, the Ming Dynasty: (a) a few quartz in glaze, many dissociative quartz particles in body, (b) a dense interaction layer of short column-like crystals at body–glaze boundary and (c) EDS spectrum of the crystal in the interaction layer, belonging to anorthite and potassium feldspar.

the bodies of every period through the Song to Qing Dynasties. The white porcelain of the Song Dynasty does not have body–glaze interaction layer, owing to the limitation of the dynamic conditions. The fast cooling process of dragon kiln does not provide enough time-interval for crystal precipitation at the body–glaze boundary. The white porcelain of the Qing Dynasty does not have body–glaze interaction layer either, in this case chemical composition limitation is decisive. Since both body and glaze have the lowest Al_2O_3 and the highest SiO_2 in the Qing Dynasty, as reported in the part I of the article, the composition of the glaze in the body–glaze boundary area could not attain supersaturation for feldspars precipitation mainly because of the shortage of Al_2O_3.

The column-like or short column-like crystals in the body–glaze boundary areas of the Ming samples and some of the Yuan samples belong to potassium feldspar $KAlSi_3O_8$ and anorthite

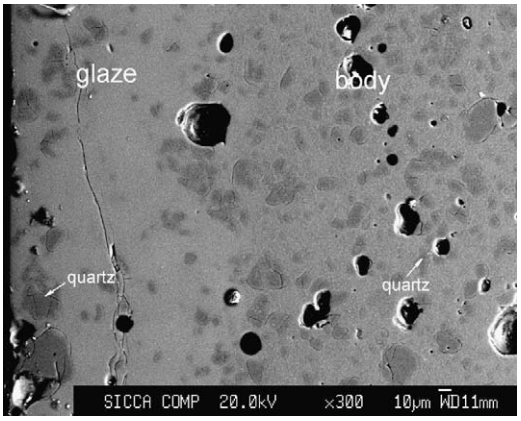

Fig. 7. SEM image of the cross-section of white porcelain 7-13 from Xingjiao kiln site, the Qing Dynasty. Many quartz particles in glaze, many dissociative quartz particles in body.

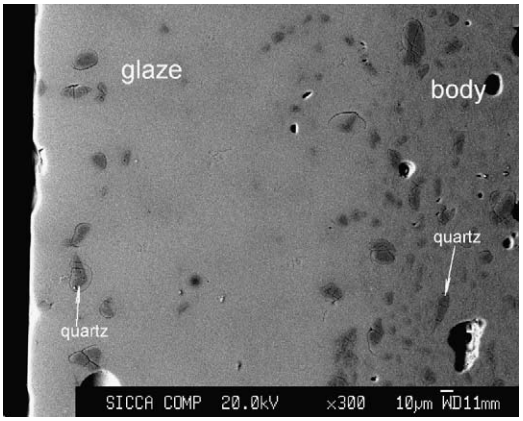

Fig. 8. SEM image of the cross-section of white porcelain 7-14 from Xingjiao kiln site, the Qing Dynasty. Many quartz particles in glaze, many dissociative quartz particles in body.

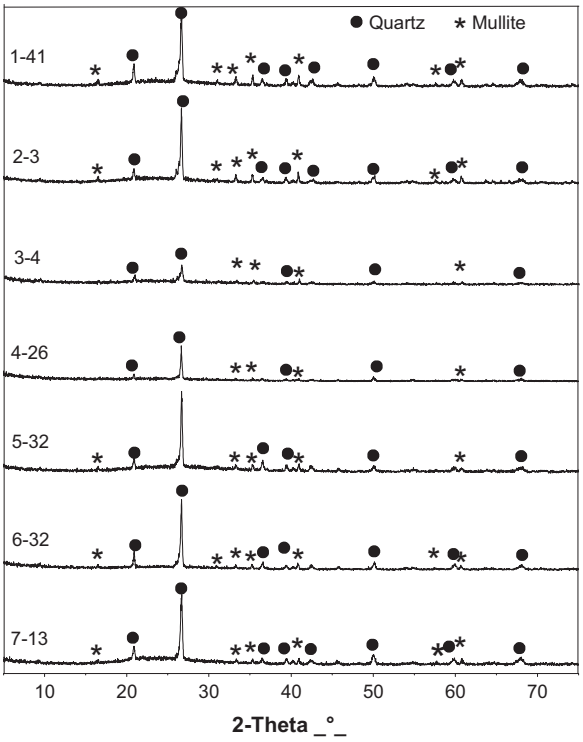

Fig. 9. XRD curves of Dehua bodies.

$CaAl_2Si_2O_8$. Al^{3+} ion in body will diffuse to glaze at high temperature, resulting in the enhancement of Al^{3+} ion content of the body-adjacent glaze, attaining the supersaturation of feldspars during cooling. The body–glaze interface provides a surface for heterogeneous nucleation, which effectively decreases the potential barrier for nucleation. The nucleation rate is decided by the supercooling degree and viscosity of the melt. The bigger the supercooling degree, the higher the amount of crystal nucleus created per unit time and per unit volume. The higher the melt viscosity, the lower the nucleation rate. Crystal growth rate is controlled by the diffusion process which changes with the composition and supercooling degree of the melt. The crystals at body–glaze boundary grow and extend to the interior of glaze according to a certain orientation.

Comparatively speaking, Dehua glaze of the Ming Dynasty has high K_2O and low CaO contents (reported in the part I of the article) and the glaze melt has relatively high viscosity at a high temperature, making it difficult for the crystals to grow to a large scale. The crystals are small and closely spaced at a high supercooling degree. The actual firing process greatly differs from the thermodynamic equilibrium state, thus the firing temperature schedules and atmosphere have a great influence on the formation of microstructure. The slow cooling rate of the chamber dragon kiln lays a technological foundation for the formation of a dense body–glaze interaction layer. Being scatterers in the submicron and micron size range, feldspar microcrystals in the interaction layer and bubbles in the glaze create full-waveband reflection and refraction upon the incident light, responsible for the translucency of the glaze layer. There is a few or no crystals at the body–glaze boundary of the glaze of the Yuan Dynasty, probably due to the fast cooling rate of the kiln.

As confirmed by XRD curves, quartz and mullite are main crystalline phases in Dehua bodies (Fig. 9). TEM images (Figs. 10 and 11) also demonstrate the existence of large amounts of unmelted quartz particles, glass and secondary mullite crystals in Dehua white ware bodies. The principal constituents in Dehua body of the Ming Dynasty can be roughly represented with the K_2O–Al_2O_3–SiO_2 ternary system. K_2O, Al_2O_3 and SiO_2 form large amounts of glass phase due to the high average K_2O content of 6.42 wt.%. Secondary mullite precipitates from the supersaturated melt during cooling. Melting rims can be observed around the quartz particles.

To show the glaze compositions more directly, 5 fluxes including Na_2O, K_2O, CaO, MgO and Fe_2O_3 are merged into R_xO_y, approximately regarded as CaO content. As marked in the SiO_2–CaO–Al_2O_3 ternary equilibrium phase diagram (Fig. 12), the glaze composition points are not located in the primary crystalline phase region of anorthite, but mainly in the primary crystalline phase region of tridymite or mullite, a few in the primary crystalline phase region of cristobalite, possessing thermodynamic qualification for the crystallization of tridymite, mullite or cristobalite. But limited to the un-equilibrium thermodynamic conditions during the firing process, no crystal precipitates from the glazes which turn out to be vitreous and homogenous. However for the body–glaze boundary area, the situation is different. Due to the diffusion of Al^{3+} ion from body to glaze at a high temperature, the glaze composition of the boundary area moves to the direction of Al_2O_3 corner of the SiO_2–CaO–Al_2O_3 equilibrium phase diagram, a majority of the Yuan and Ming boundary glazes and a part of the Song boundary glazes enter the primary crystalline phase region of anorthite, which is the thermodynamic basis for the formation of a body–glaze interaction layer. Moreover, whether a reaction layer can really form, dynamic conditions are essential.

Based on the thermodynamics, glass has bigger internal energy than the corresponding crystallized substance, crystalline state is more stable than vitreous state; therefore, there always exists a tendency to transform into crystalline state from vitreous state. But the phase transformation process does not happen spontaneously. In the area of phase transformation, atoms must realign according to the structure of the new phase. Nucleation generally occurs with much more difficulty in the interior of a uniform substance, by a process called homogeneous nucleation. The creation of a nucleus implies the formation of an interface at the boundaries of a new phase. Heterogeneous nucleation occurs much more often than homogeneous nucleation. It forms at preferential sites such as phase boundaries or impurities and requires less energy than homogeneous nucleation. The barrier energy for heterogeneous nucleation is reduced, and less supercooling is needed. In this case, heterogeneous nucleation happens at body–glaze interface, followed by the stage of fast crystal growth at a certain temperature and supercooling condition.

As for the microstructures of the Dehua white porcelains of the Song, Yuan, Ming and Qing Dynasties, each has its own

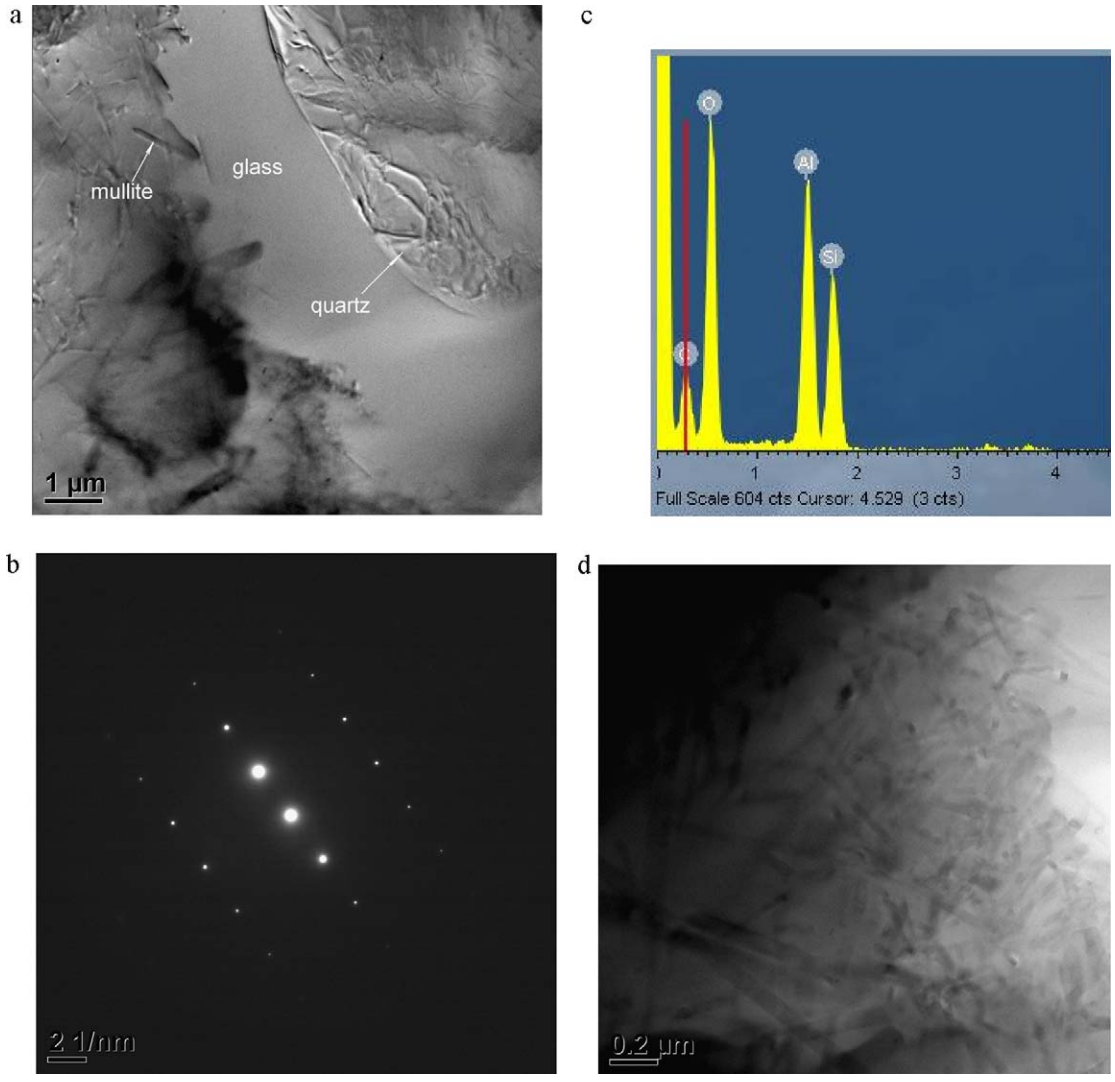

Fig. 10. TEM images of white porcelain 2-3 from Zulonggong kiln site, the Ming Dynasty: (a) quartz, glass and secondary mullite in the body, (b) SAD pattern of a quartz single crystal, (c) EDS spectrum of secondary mullite, and (d) needle-like secondary mullite.

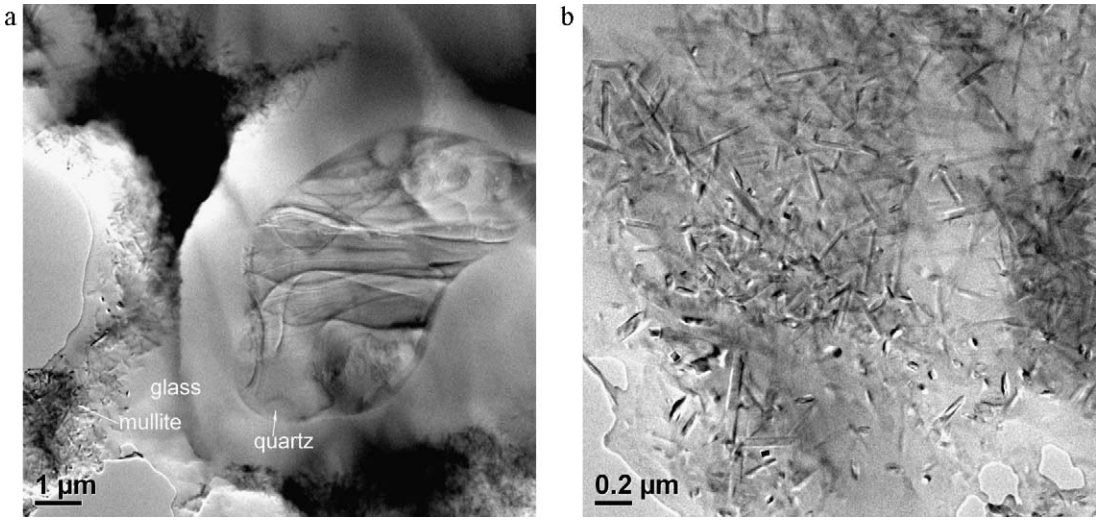

Fig. 11. TEM images of white porcelain 4-10 from Jiabeishan kiln site, the Ming Dynasty: (a) quartz, glass and secondary mullite in the body and (b) needle-like secondary mullite.

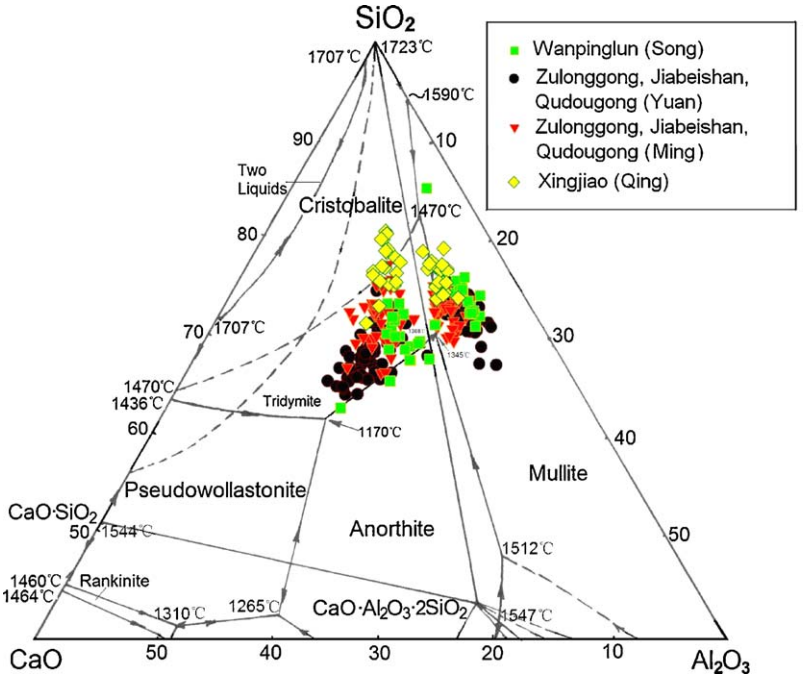

Fig. 12. Position of the composition points of Dehua glazes in $CaO–Al_2O_3–SiO_2$ equilibrium phase diagram.

characteristics, reflecting the differences of compositions and processing techniques, also indicating the difference of firing techniques. Moreover, the microstructure characteristics can serve as an assistant judging criterion for Dehua white porcelains of different periods.

3.2. Firing temperature and physical properties of Dehua white porcelain

Fig. 13 shows the whiteness of Dehua white porcelain. The samples for test cover all the visual characteristics including greenish-white, grayish-white, yellowish-white and ivory-white. Except for the two samples from Xingjiao kiln site, the Hunter whiteness of all the rest samples is between 70 and 87, which has reached quite a high level of whiteness. Fig. 14 gives the spectral reflectance curves of the typical Dehua white porcelains. The Ming samples selected are ‘‘ivory-white’’ porcelains. The ‘‘ivory-white’’ samples have the highest visible light reflectance, showing the best gloss. The ‘‘ivory-white’’ reflectance curves are upward with no peaks, long-wave light is reflected more than short-wave light. The majority of Song, Yuan and Qing samples turn out to be pale greenish white or grayish white, having a downward tendency in long-wave light reflectance.

Firing temperatures and properties of the samples are listed in Table 2. As for the well-fired Dehua bodies, water absorption is less than 0.9% with the exception of two cases, where it is 1.5% and 2.0% respectively, apparent porosity is generally 1%, bulk density is higher than 1.90 g/cm^3, bending strength is between 53.6 MPa and 92.9 MPa, firing temperature is between 1240 °C and 1390 °C. Firing temperatures of the Ming and Qing bodies are lower than those of the Song and Yuan bodies, because the Ming and Qing bodies have higher flux contents.

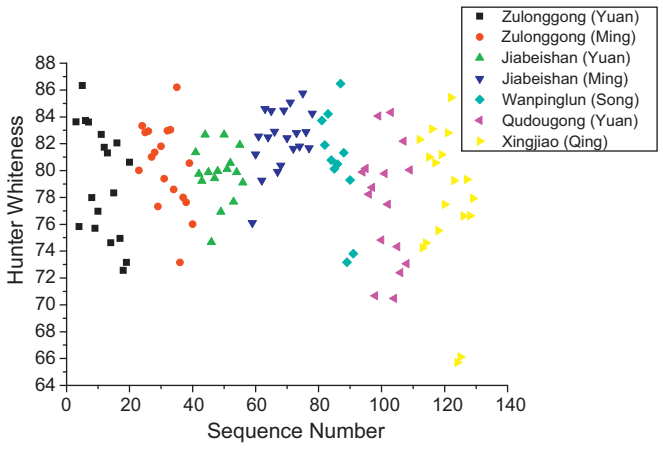

Fig. 13. Whiteness of Dehua white porcelains.

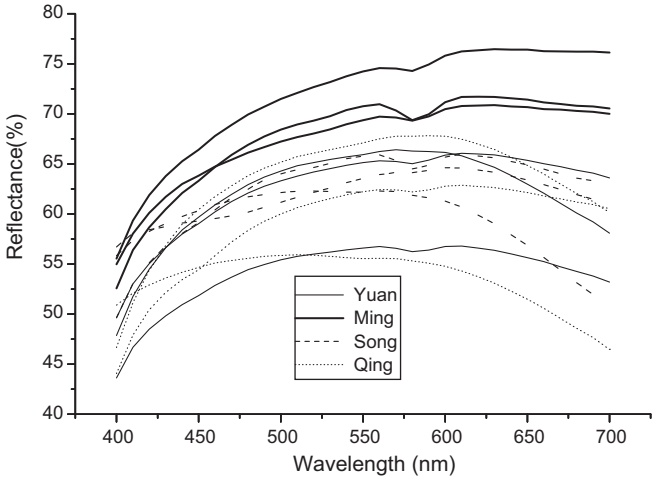

Fig. 14. Spectral reflectance curves of the typical Dehua white porcelains.

Table 2
Firing temperatures and physical properties of Dehua bodies.

Number	Time	Kiln site	Bending strength (MPa)	Bulk density (g/cm^3)	Water absorption (%)	Apparent porosity (%)	Firing temperature (°C)
5-2	Song	Wanpinglun	66.5	2.21	0.5	1	1330
5-12	Song	Wanpinglun	53.6	2.21	0.9	2	1380
5-32	Song	Wanpinglun		2.19	0.8	2	1330
5-35	Song	Wanpinglun		2.22	0.6	1	
5-48	Song	Wanpinglun		2.32	0.6	1	
1-1	Yuan	Zulonggong	85.8	2.34	0.4	1	1350
1-3	Yuan	Zulonggong	64.9	2.23	0.5	1	1300
1-22	Yuan	Zulonggong		2.30	0.4	1	
1-41	Yuan	Zulonggong		2.32	2.0	5	1310
1-50	Yuan	Zulonggong		2.21	0.6	1	
3-4	Yuan	Jiabeishan	73.8	2.22	0.7	1	1380
3-5	Yuan	Jiabeishan		2.24	0.9	2	
3-10	Yuan	Jiabeishan	76.0	2.29	0.6	1	1350
3-25	Yuan	Jiabeishan		2.37	0.6	1	1390
6-17	Yuan	Qudougong		2.36	0.5	1	1330
6-32	Yuan	Qudougong	76.0	2.27	0.5	1	1320
6-39	Yuan	Qudougong		2.33	0.4	1	
6-44	Yuan	Qudougong	81.0	2.37	0.4	1	1340
6-49	Yuan	Qudougong		2.32	0.5	1	1290
2-3	Ming	Zulonggong	75.4	2.31	0.3	1	1260
2-6	Ming	Zulonggong	74.7	2.24	0.5	1	1320
2-9	Ming	Zulonggong		2.31	0.4	1	
2-25	Ming	Zulonggong		2.34	0.3	1	
4-8	Ming	Jiabeishan		2.27	0.6	1	1280
4-10	Ming	Jiabeishan	82.5	2.23	0.5	1	1250
4-15	Ming	Jiabeishan	92.9	2.32	0.4	1	1280
4-22	Ming	Jiabeishan		2.17	0.5	1	1250
4-48	Ming	Jiabeishan		1.90	1.5	3	1240
7-2	Qing	Xingjiao		2.40	0.2	1	
7-13	Qing	Xingjiao	81.5	2.30	0.4	1	1280
7-14	Qing	Xingjiao	63.4	2.27	0.4	1	1310
7-15	Qing	Xingjiao		2.26	0.4	1	1280
7-16	Qing	Xingjiao		2.22	0.5	1	

In brief, judged from the data in Table 2, the well-fired Dehua white porcelains have reached quite a high level of quality, being comparable to modern porcelains.

4. Conclusion

As for the microstructures of the Dehua white porcelains of the Song, Yuan, Ming and Qing Dynasties, each has its own characteristics, reflecting the differences of compositions and processing techniques, also indicating the difference of firing techniques. Moreover, the microstructure characteristics can serve as an assistant judging criterion for Dehua white porcelains of different periods.

There are large amounts of unmelted quartz particles, glass and secondary mullite crystals in Dehua white ware bodies of every period through the Song to Qing Dynasties.

There are no or just a few un-melted dissociate quartz crystals in the glaze of the Song, Yuan and Ming Dynasties, indicating that the technique for elutriating the glaze-used porcelain stones is rather fine during that time. But the elutriation technique is quite rough in the Qing Dynasty, many dissociative quartz particles with melting rims can be observed in glaze layers.

A dense body–glaze interaction layer of short-column like feldspar microcrystals (potassium feldspar and anorthite) can be observed in the ‘‘ivory-white’’ sample of the Ming Dynasty. Being scatterers in the submicron and micron size range, feldspars in the interaction layer and bubbles in the glaze create full-waveband reflection and refraction upon the incident light, responsible for the translucency of the glaze layer.

Liquid–liquid phase-separation structure can be found in some samples within the interspaces of crystals of the body–glaze interaction layer.

Judged from the physical properties of Dehua ware body including water absorption, apparent porosity, bulk density, bending strength and firing temperature, the well-fired Dehua white porcelains have reached quite a high level of quality, being comparable to modern porcelains.

Acknowledgment

This work was supported by ‘‘Compass’’ project 20080305 of China State Administration for Cultural Heritage.

Reference

[1] GB/T 3810.3, Testing Methods for Ceramic Tiles, Part 3: Testing of Water Absorption, Apparent Porosity, Apparent Relative Density and Bulk Density, 1999.